https://doi.org/10.5607/en.2018.27.1.16
Exp Neurobiol. 2018 Feb;27(1):16-27.
pISSN 1226-2560 • eISSN 2093-8144

Original Article

Experimental Neurobiology

Functional Analysis and Immunochemical Analyses of Ca^{2+} Homeostasis-related Proteins Expression of Glaucoma-induced Retinal Degeneration in Rats

Ji-Yeon Lee and Su-Ja Oh*

Department of Anatomy, College of Medicine, The Catholic University of Korea, Seoul 06591, Korea

The retinal degeneration resulting from elevated intraocular pressure was evaluated through functional and morphological analyses, for better understanding of the pathophysiology of glaucoma. Ocular hypertension was induced via unilateral episcleral venous cauterization in rats. Experimental time was set at 1 and 3 days, and 1, 2, 4, and 8 weeks post-operation. Retinal function was analyzed using electroretinography. For morphological analysis, retinal tissues were processed for immunochemistry by using antibodies against the calcium-sensing receptor and calcium-binding proteins. Apoptosis was analyzed using the TUNEL method and electron microscopy. Amplitudes of a- and b-wave in scotopic and photopic responses were found to be reduced in all glaucomatous retinas. Photopic negative response for ganglion cell function significantly reduced from 1-day and more significantly reduced in 2-week glaucoma. Calcium-sensing receptor immunoreactivity in ganglion cells remarkably reduced at 8 weeks; conversely, protein amounts increased significantly. Calcium-binding proteins immunoreactivity in amacrine cells clearly reduced at 8 weeks, despite of uneven changes in protein amounts. Apoptosis appeared in both photoreceptors and ganglion cells in 8-week glaucomatous retina. Apoptotic feature of photoreceptors was typical, whereas that of ganglion cells was necrotic in nature. These findings suggest that elevated intraocular pressure affects the sensitivity of photoreceptors and retinal ganglion cells, and leads to apoptotic death. The calcium-sensing receptor may be a useful detector for alteration of extracellular calcium levels surrounding the ganglion cells.

Key words: electroretinography, Ca^{2+}-sensing receptor, retinal ganglion cell, apoptosis, glaucoma, rats

INTRODUCTION

Glaucoma, a group of optic neuropathies, is the leading neurodegenerative cause of blindness [1]. It is commonly characterized by a slow progressive degeneration of the axon and then the soma of retinal ganglion cells [2, 3]. Among patients with diverse glaucoma types worldwide, primary open-angle glaucoma with elevated intraocular pressure (IOP) is the most common; however, the prevalence of normal tension glaucoma with IOP in the normal range is increasing [4]. The pathogenesis of glaucomatous optic neuropathies is therefore most likely explained by two distinct mechanisms, the mechanical or pressure theory and the vascular theory [5, 6]. IOP has been confirmed as the only treatable risk factor for glaucoma till now. Elevated IOP contributes to progressive

Received December 23, 2017, Revised February 1, 2018,
Accepted February 12, 2018

*To whom correspondence should be addressed.
TEL: 82-2-2258-7259, FAX: 82-2-536-3110
e-mail: sujaoh@catholic.ac.kr

damage of the axon and soma of retinal ganglion cells and eventually to visual field loss [3, 7]. Non-IOP-related mechanisms such as vascular abnormality may play an important role in the pathogenesis of normal tension glaucoma.

It is widely accepted that if glaucoma is recognized in its early stages, subsequent visual loss can be limited or prevented via currently available treatments. Most cases of glaucoma, however, given its clinically subtle early signs, are not disclosed until vision has already been irreversibly lost [3]. Currently, efforts are being made to screen glaucoma's underlying mechanisms and other treatable risk factors, aiming to enable early diagnosis and detection.

Thereby, the present study aims to discover crucial episodes useful in early detection of glaucoma, focusing on the retina itself. For this, the spatiotemporal sequence of retinal degeneration caused by elevated IOP was functionally and morphologically assessed. We used a rat model of primary open-angle type chronic glaucoma induced via unilateral episcleral venous cauterization, according to the diagnostic criterion that primary open-angle glaucoma is a chronic, generally bilateral, but asymmetrical disease [3]. Functional assessment through flash electroretinography (ERG) was conducted to detect alteration in the electric reactivity of the conducting neurons in the photo-transduction pathway in the glaucomatous retinas: that of both photoreceptors and ON bipolar cells was evaluated based on changes in a- and b-wave amplitudes [8-11], and that of the RGCs based on changes in photopic negative responses (PhNRs) [10, 11]. Morphological assessment of retinal degeneration was largely performed via immunochemical analyses using Ca^{2+} homeostasis-related proteins, such as calcium-binding proteins and the calcium-sensing receptor.

The divalent cation Ca^{2+} works as a secondary messenger in many signaling pathways, such as membrane excitability and synaptic transmission, in the central nervous system including the retina [12]. Calcium-binding proteins (CaBPs) bind calcium to increase the cell's buffering capacity as a constituent of the termination mechanisms of intracellular calcium signal, including calcium buffering, extracellular extrusion, and intra-organelle sequestration. CaBPs are usually expressed in a cell-specific manner and thereby used for identification of specific neuronal types, especially types of amacrine cells, a type of associated retinal neuron. In our study, the immunochemical characteristics of CaBPs were utilized for determining changed amacrine cells in glaucomatous retinas, in addition to indistinct oscillatory potentials in flash ERGs. The calcium-sensing receptor (CaSR), as a member of the G-protein-coupled receptor C family, is activated by local extracellular Ca^{2+} or by other physiologically relevant polycationic molecules as a first messenger, and therefore currently accepted to play a role in maintaining local ionic homeostasis in the brain [13, 14]. Despite ubiquitous distribution of CaSR in the brain [15], there is nearly no report on CaSR expression in the retina. We demonstrate, using immunochemical analysis, CaSR expression in the retinal ganglion cells and its alteration pattern under ocular hypertension, followed by electron microscopy of CaSR-immunostained retinal preparation for the identification of apoptotic retinal ganglion cell death in glaucomatous retinas.

MATERIALS AND METHODS

Animals

Sprague-Dawley rats aged 8 weeks were used. All experimental procedures complied with the regulations of the Catholic Ethics Committee of the Catholic University of Korea, which conforms to the US National Institute of Health (NIH) guidelines for the Care and Use of Laboratory Animals (NIH Publications No. 80-23), revised in 1996. Animals were maintained at a 12 h light/dark cycle and fed standard chow.

Elevation of IOP

Elevated IOP was induced via venous cauterization. Briefly, animals were anesthetized with a mixture of tiletamine plus zolazepam (Zoletil; Virbac, France) /xylazine hydrochloride (Rompun; Bayer, Germany) (50/15 mg/kg ip injection). Proparacaine (0.5% concentration) was topically eye-dropped. Three of four episcleral veins in the right-side eyeball were cauterized with a 30-gauge tip cautery (Bovie Medical Co., USA) under a surgical microscope (Olympus, Tokyo, Japan). Animals were grouped and cared for 1 and 3 days, and 1, 2, 4, and 8 weeks after operation. Twenty animals each were assigned for each experimental time point and, 15 animals for normal control and 5 animals for aged-matched control.

IOP measurements

IOP was cumulatively measured using a rodent tonometer, TonoLab (Tono-Pen XL®, Medtronic Solan, Jacksonville, FL, USA) in glaucoma and contralateral control eyes at all time points after operation. Five consecutive readings via a single measurement were averaged and corrected based on a linear equation obtained from IOP calibration with the pressure transducer. Data were analyzed by averaging the IOP measurements for each time point.

ERG recording

Rats were dark-adapted overnight before ERG recordings. Under dim red light, rats were anesthetized with intraperitoneal injection of zolazepam and xylazine, and placed in a Ganzfeld dome laying on the stage to ensure a stable position for recording. After moistening with a hydroxypropyl methylcellulose gel, gold-ring

contact-lens electrodes were placed on the eyes and, two reference electrodes and one ground electrode, subcutaneously in the ears and in the tail, respectively. ERGs were recorded with a universal electrophysiological system (UTAS-3000 MF; LKC Technologies, Gaithersburg, MD, USA). Luminescence intensity was calibrated by the manufacturer and controlled by computer system. Scotopic and photopic ERG responses were each obtained from both eyes simultaneously. Scotopic responses are the mechanisms that are specifically adapted for dim or night vision [16]. Rats were first tested for rod-mediated scotopic ERG under dark adaptation exposed to flash intensity of 0.99 cd·s/m^2. To obtain photopic responses, light-adapted rods with a saturating background (30 cd·s/m^2) for 10 min presented flashes of intensity of 75.36 cd·s/m^2 (4 dB). For each condition, 3~5 responses to the flash stimuli were averaged, with a stimulus interval of 15 s. A-wave amplitude was measured from the baseline to the maximum a-wave peak, and that of b-wave, from the maximum a-wave peak to the maximum b-wave peak. PhNR was recorded under stimulus conditions: a brief 0 dB blue flash (peak wavelength 470 nm) at an intensity of 10 cd/m^2 against a blue background (peak wavelength 470 nm) of 10 cd/m^2 (photopic units). PhNR amplitude was measured from the baseline to the trough of the negative peak following the b-wave. The peak latency of the PhNR was measured as the elapsed time between the instant of the flash and the point of maximal descent following the b-waves.

Tissue preparation

Eyeballs were enucleated under anesthesia with 4% chloral hydrate. The posterior halves of the globes were immersed in 4% paraformaldehyde in 0.1 M phosphate buffer (PB), pH 7.4. Whole retinas were dissected and immersed in the same fixative for 2 h. After fixation, retinas were immersed in 30% sucrose, refrigerated overnight, and then flash-frozen in liquid nitrogen and stored at -70°C for preservation.

Immunohistochemistry

Retinal pieces were trimmed out from the central portion of the superior quadrant and rinsed with 0.01 M phosphate buffered saline (PBS), pH 7.4. After thorough rinsing, retinal pieces were embedded in 4% agar and cut into 40-μm-thick vertical sections. The retinal sections were collected in culture wells and processed for immunofluorescent microscopy. To block nonspecific binding sites, sections were treated with buffer B (1% BSA, 0.2% gelatine bovine, 0.05% saponin/in PBS) for 3 h on ice. Sections were then incubated with antibodies against monoclonal mouse anti-Calcium Sensing Receptor (CaSR, Sigma-Aldrich, St.Louis, MO, USA; dilution 1:3000) and one of following antibodies: polyclonal rabbit anti-calbindin D28K (Swant, CH-1723 Marlyl, Switzerland; dilution 1:2000), polyclonal rabbit anti-calretinin (Millipore, Temecula, CA, USA; dilution 1:5000), polyclonal rabbit anti-parvalbumin (Swant; dilution 1:5000) overnight at 4°C. Immunoreactivity was visualized with Alexa Fluor 488 donkey anti-mouse and rabbit conjugated IgG (Life technologies, Grand Island, NY, USA; dilution 1:2000). After rinsing in PBS, sections were mounted on a glass slide with mounting medium.

Confocal microscopy

Immunofluorescent staining was evaluated via confocal laser-scanning microscopy (LSM 510 Meta, Carl Zeiss Co. Ltd., Germany). Fluorescent images were captured with green laser (excitation 488 nm, emission 490~555 nm) at 400× magnification power. Captured images were converted to JPEG.

Western blot analysis

Western blotting was performed on homogenized retinal extracts. Protein concentration in each sample was assayed using the Pierce™ BCA protein assay. Duplicate sets of protein standards containing 0, 0.05, 0.1, 0.2, 0.25, 0.5 and 1 mg/ml BSA were assayed using the same method. Tissue-sample aliquots corresponding to 25 μg of total protein were heated at 100°C for 10 min with an equivalent volume of 2× sample buffer (containing 4% SDS and 10% mercaptoethanol) and loaded onto 5~12% SDS-polyacrylamide gels. The proteins were electro-transferred onto a polyvinylidene difluoride membrane in Tris-glycine-methanol buffer and treated for 1 h in a blocking solution. The membrane was then incubated with antibodies in the blocking solution overnight at 4°C. Primary antibodies were the same as those used in immunohistochemistry; mouse monoclonal anti-β-actin (Sigma-Aldrich, dilution 1:100,000) was used as the control. The antibody-treated membrane was rinsed with 0.1% Tween-20 in PBS for 30 min, and then, incubated with biotinylated donkey anti-mouse IgG or anti-rabbit IgG (Vector Laboratories, Burlingame, CA, USA; dilution 1:1,000) for 2 h. The blot was washed, processed for analysis using an enhanced chemiluminescence (ECL) detection kit (Amersham, Arlington Heights, IL, USA), and visualized using Fujifilm Image Reader LAS-4000 (Fujifilm, Tokyo, Japan). Each experiment was repeated at least thrice, and representative blots are shown. Densitometric analysis was performed using Multi Gauge V3.0 (Fujifilm). Data are presented as mean±SE and statistical significance was determined using Student's t-test.

Terminal deoxynucleotidyl transferase dUDT nick end labeling (TUNEL) assay

Apoptosis was evaluated using the TUNEL method. Retinal

https://doi.org/10.5607/en.2018.27.1.16

sections (40-μm-thick) were embedded in 4% paraformaldehyde, washed and stained (In Situ Cell Death Detection Kit, Fluorescein; Roche Applied Science, Mannheim, Germany). Briefly, after washing with PBS for 30 min, sections were incubated with 0.1% Triton X-100 / 0.1% sodium citrate solution for 2 min on ice for better permeability. Sections were then incubated with terminal dUDT enzyme at 37°C for 1 h for tailing reaction, and counterstained with 4',-6-diamidino-2'-phenylindole (DAPI) for cell nuclei. The reaction was examined using a confocal microscope (LSM 510 Meta).

Electron microscopy

To examine the ultrastructure of normal and 8-week glaucoma retinas, CaSR-immunostained retinal sections were fixed with 2.5% glutaraldehyde (in PB), washed with PB, and post-fixed with 1% osmium tetroxide (in PB). Sections were then washed with PB and dehydrated in an ethanol gradient. After dehydration, sections were infiltrated with Epon 812, flat-mounted on transparent film, and polymerized by curing at 60°C. Ultrathin sections (70~90 nm thickness) were collected on a one-hole grid and the ultrastructure was observed using an electron microscope (JEM-1010; JEOL, Tokyo, Japan).

RESULTS

IOP was elevated to 20 mmHg on the first day after operation and thereafter sustained in the range of 17~20 mmHg throughout the experiment (Fig. 1). IOP and ERG were cumulatively surveyed throughout all experimental time points to elucidate the temporal correlation between IOP elevation and functional damage on each component of ERG. Immunochemical changes were studied at the given time points from 1 week post-operation for spatial correlation between elevated IOP and its morphological impact on specific neuronal populations.

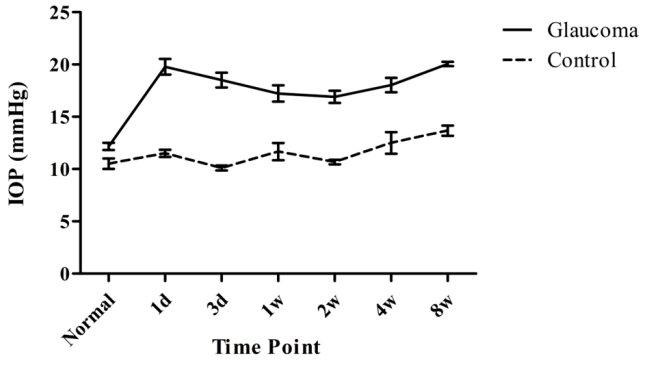

Fig. 1. IOP is temporally profiled in glaucoma and contralateral control eyes. After cauterization, IOP of glaucoma eyes is remarkably higher than that of control eyes. Data are presented as means±SE: n=10 for control and each glaucoma value.

Electroretinography (ERG) of scotopic responses

ERG recordings of scotopic responses in glaucoma were depicted together with that of a normal retina aged 8 weeks (Fig. 2). In all time points, ERGs of scotopic response in glaucoma retinas showed clear reduction in a- and b-wave amplitudes compared to those of normal retina. Oscillatory potentials before the b-wave peak, even though very slight, were also reduced. At 8 weeks post-operation, ERG of glaucoma retinas showed reduced amplitudes than that of normal retina.

ERG of photopic responses

ERG recordings of photopic responses in glaucoma retinas were compared at all time points with those of normal retina (Fig. 3). ERGs of photopic responses in all retinas showed negligible a-wave amplitudes and oscillatory potentials. However, b-wave amplitude in glaucoma retinas was slightly reduced at 1 and 3 days, thereafter slightly recovered and sustained.

Photopic negative responses (PhNRs)

PhNRs in glaucoma retinas were compared with those in normal control retina at each time point (Fig. 4a). PhNRs amplitude in glaucoma retinas significantly reduced from 1 day, recording the lowest at 2 weeks ($p<0.01$), to 8 weeks ($p<0.05$) (Fig. 4b).

CaSR and CaBPs immunoreactivity

CaSR strongly immunolocalized into the neurons in the ganglion cell layer (GCL) and nonspecifically into both the neurons in the inner nuclear layer (INL) and the rod and cone layer at normal state (Fig. 5a). CaSR immunoreactivity in the GCL showed no large change in 1-week glaucoma retina, but clearly reduced after 2-week glaucoma especially in ganglion cells (Fig. 5b~d). Calbindin immunolocalized into the horizontal cells in the outermost part of the INL, into the amacrine cell soma in the inner half of the INL and their ramifying processes in the inner plexiform layer (IPL), and to the displaced amacrine and ganglion cells in the GCL (Fig. 5e). Calbindin immunoreactivity showed no large change in 1- and 2-week glaucoma (Fig. 5f and g); however, it remarkably reduced in 8-week glaucoma in all immunoreactive neuronal types (Fig. 5h). Calretinin immunolocalized into the amacrine cells in the INL and their processes ramified in three laminae in the IPL, and into the neurons in the GCL (Fig. 5i). In 1- and 2-week glaucoma, there was no large change in calretinin immunoreactivity (Fig. 5j and k), but calretinin immunoreactive amacrine cells and neurons in the GCL slightly reduced in cell number and immuno-

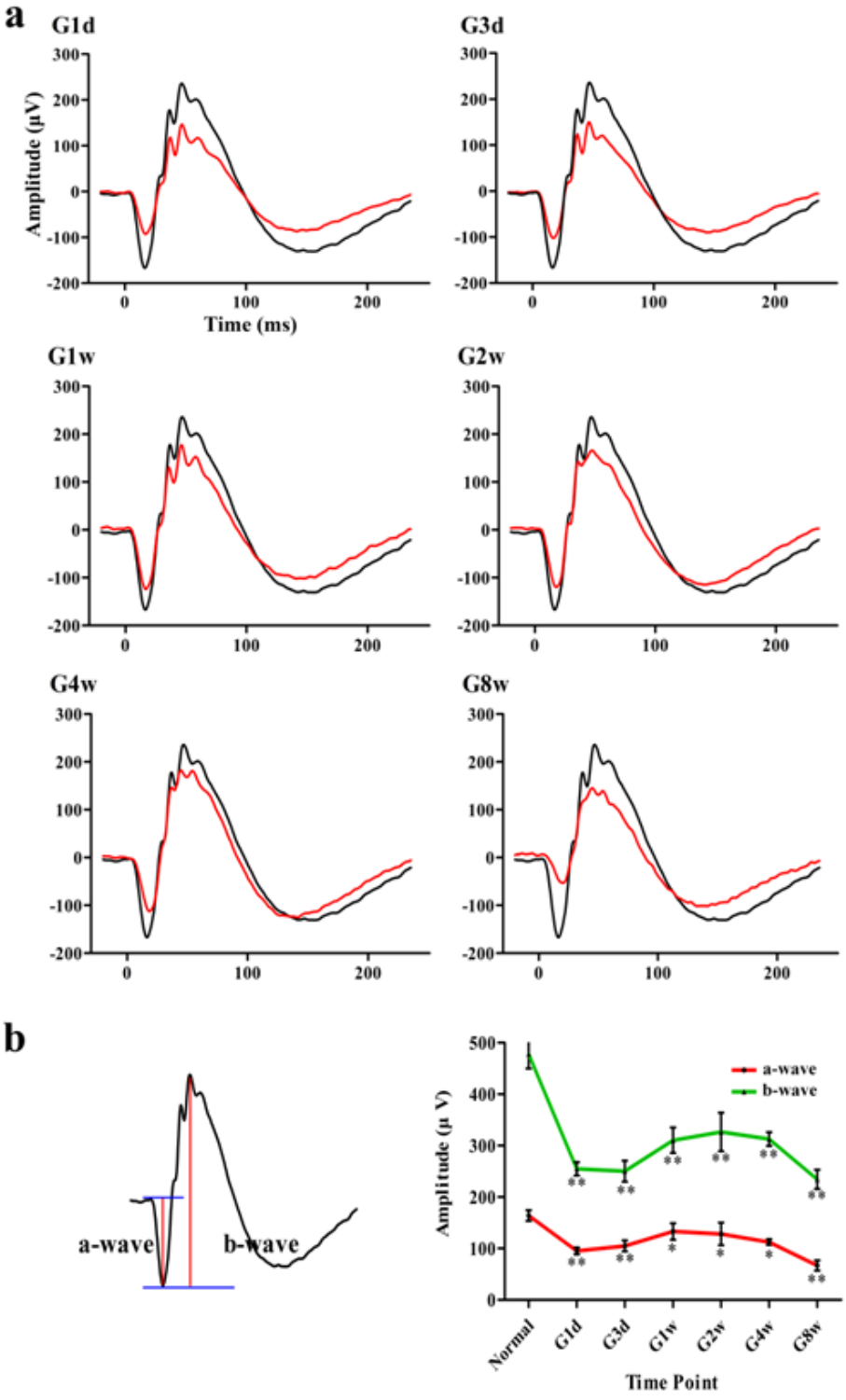

Fig. 2. Scotopic ERGs were evaluated. In (a), representative ERGs of glaucoma (G, red colored waveforms) at each time point (G1d, G 1day; G3d, G 3day; G1w, G 1week; G2w, G 2week; G4w, G 4week and G8w, G 8week) are compared with that of normal control retina (Normal, black colored waveform). In (b), a- and b-wave amplitudes of scotopic response in normal state were defined, and those in glaucoma retina at each time point were evaluated with a linear graph.

reactivity in 8-week glaucoma (Fig. 5l). Parvalbumin immunolocalized to AII amacrine cells in the INL and their processes in the IPL (Fig. 5m). Parvalbumin immunoreactivity in the whole-cell profile of AII amacrine cells did not reduce in 1-week glaucoma (Fig. 5n). However, immunoreactivity clearly reduced in both lobular appendages in OFF lamina of the IPL and the dendrites near the GCL after 2-week glaucoma (Fig. 5o and p).

CaSR and CaBPs expression

CaSR and CaBP expression levels were evaluated via western blot

https://doi.org/10.5607/en.2018.27.1.16

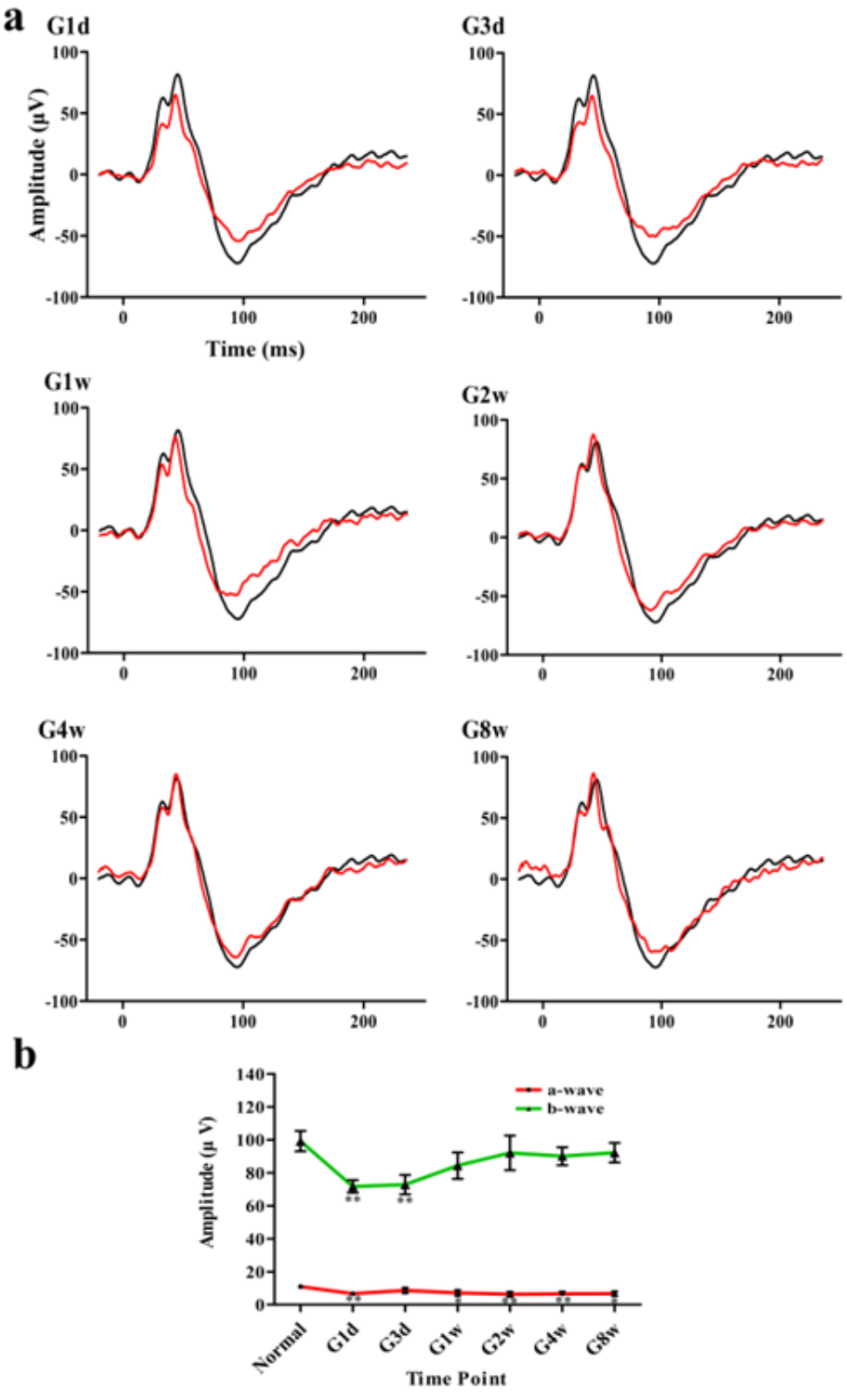

Fig. 3. Photopic ERGs were evaluated. In (a), representative ERGs of scotopic responses of glaucoma (G, red colored waveforms) at each time point (G1d, G 1day; G3d, G 3day; G1w, G 1week; G2w, G 2week; G4w, G 4week and G8w, G 8week) are compared with that of normal control retina (Normal, black colored waveform). In (b), a- and b-wave amplitudes in normal retina and glaucoma retina at each time point were evaluated with a linear graph.

in glaucomatous eyes. CaSR expression levels began to increase in 1-week glaucoma and peaked at 8 weeks (Fig. 6a and b). Changes in calbindin and calretinin expression levels present a shallow concave curve and a mild convex curve showing a bottom and a peak at 2 weeks, respectively (Fig. 6c and d). Parvalbumin expression levels showed no large change throughout the glaucomatous retinas (Fig. 6e).

Neuronal apoptosis

Neuronal apoptosis was assayed using TUNEL (Fig. 7) and

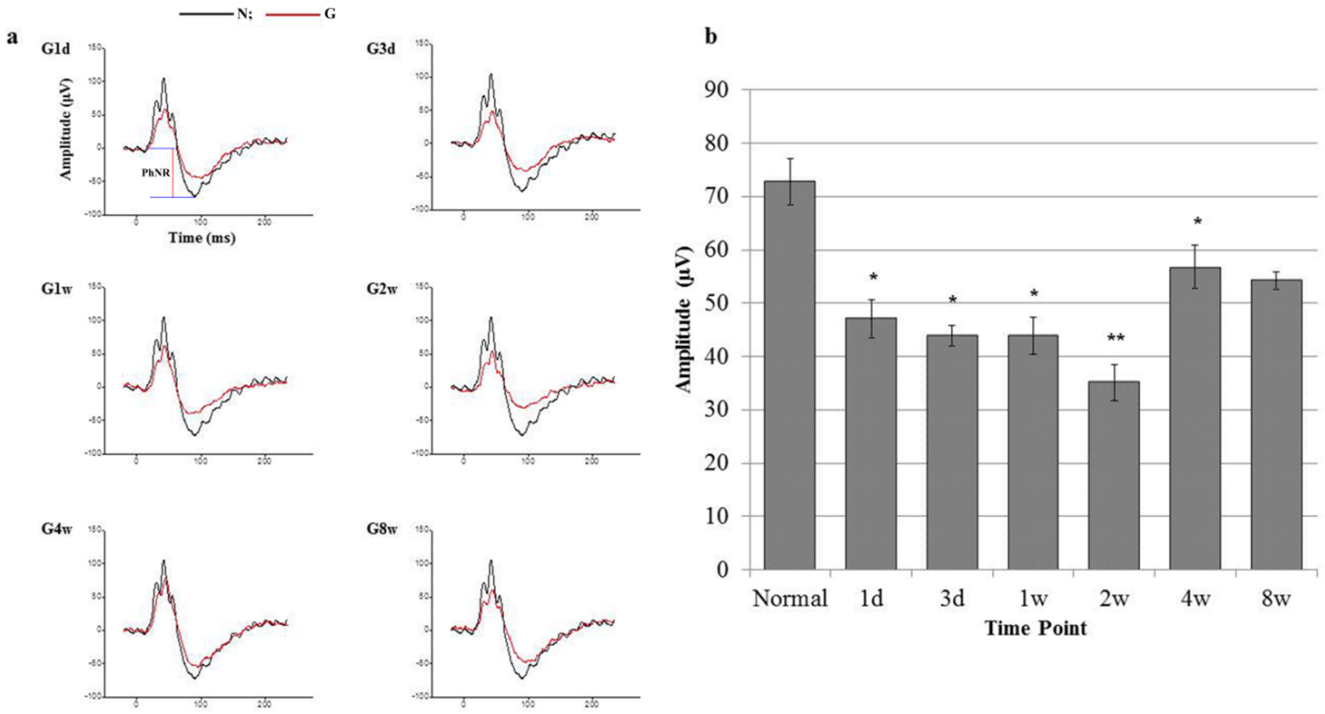

Fig. 4. Photopic negative response (PhNR) was evaluated. In (a), representative PhNRs of glaucoma retina (G) at each time point (G1d, G 1day; G3d, G 3day; G1w, G 1week; G2w, G 2weeks; G4w, G 4weeks; G8w, G 8weeks) are compared with that of normal control retina (N). In (b), PhNR amplitudes in the retinas at normal state (Normal) and at each time point of glaucoma retinas (1d, 3d, 1w, 2w, 4w, 8w) are compared. PhNR amplitude at 2 week glaucoma shows significant reduction ($p<0.01$), compared to normal retina. *$p<0.05$ and **$p<0.01$, paired Student's t-test.

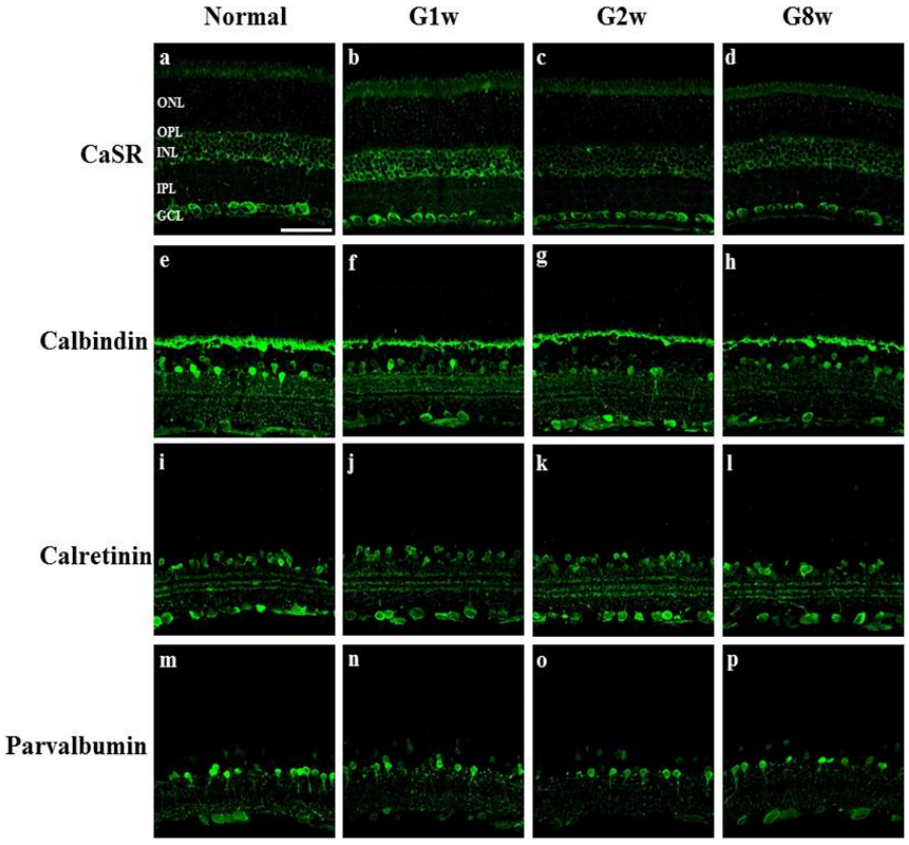

Fig. 5. Confocal microscopic analysis of normal and glaucoma retinas processed for CaSR and calcium-binding proteins immunohistochemistry. Immunohistochemistry for CaSR (a~d), calbindin (e~h), calretinin (i~l) and parvalbumin (m~p) was performed in normal retina (Normal: a, e, i, m), and in 1 week (G1w: b, f, j, n), 2 week (G2w: c, g, k, o), and 8 week (G8w: d, h, l, p) glaucoma retinas. CaSR immunoreactivity in the neurons in the ganglion cell layer (GCL) clearly reduced in G2w and G8w retinas. Calbindin immunoreactivity in amacrine cells in the inner nuclear layer (INL) gradually reduced in glaucoma retinas and that in the axons of ganglion cells increased. Calretinin immunoreactivity in amacrine cells showed no large change in glaucoma retinas. Parvalbumin immunoreactivity in the entire AII amacrine cell profile gradually reduced in glaucoma retinas. IPL, inner plexiform layer; ONL, outer nuclear layer; OPL, outer plexiform layer. Scale bar indicates 50 μm.

https://doi.org/10.5607/en.2018.27.1.16

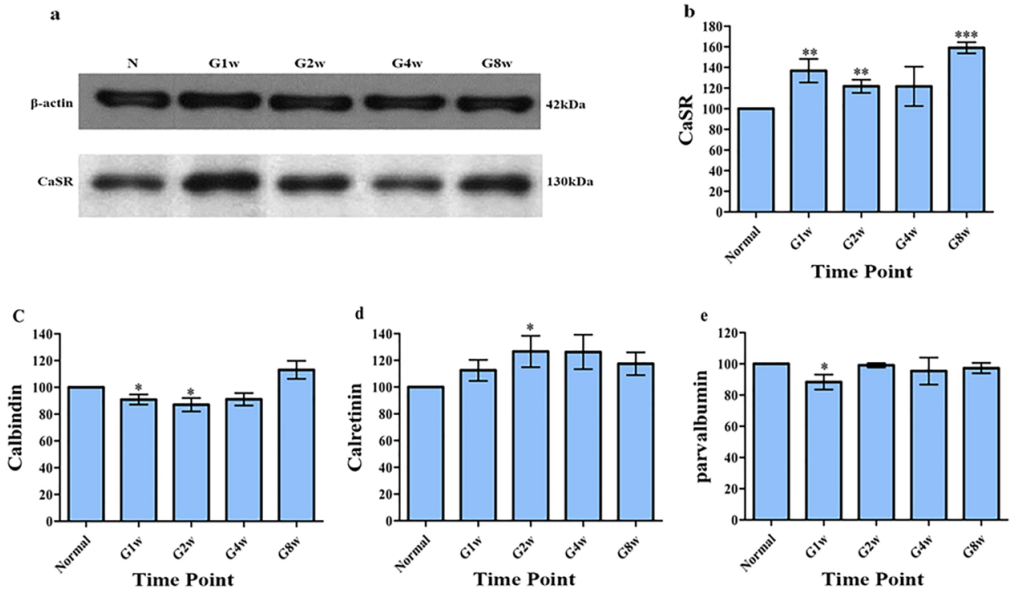

Fig. 6. Evaluation of CaSR and calcium-binding proteins (CaBPs) expression levels in glaucoma retinas. Immunoreactivity bands corresponding to β-actin (42 kDa) and CaSR (130 kDa) reveal temporal expression patterns in normal and glaucoma retinas. In (a), representative blots from normal and glaucoma retinas are shown. Densitometry measurements of CaSR (b) and CaBPs (c~e) normalized with actin as loading control for retinas are shown in accompanying graphs, n=10. *p<0.05, **p<0.01, and ***p<0.001, paired Student's t-test (normal vs. glaucoma).

electron microscopy (Fig. 8). In normal control retina and experimental control retina of 8-week glaucoma, there were no TUNEL-positive cells (Fig. 7a~d). TUNEL positivity appeared in a few photoreceptors in the outer nuclear layer (ONL) and in several ganglion cells in the GCL only in 8-week glaucoma retina (Fig. 7e and f).

In electron microscopic observation of 8-week glaucoma retina, dying photoreceptors showed the classical apoptotic feature of pyknotic nucleus (Fig. 8a). Degenerating retinal ganglion cells showed necrotic features representing the pyknotic and tortious nucleus, endoplasmic reticulum with enlarged cisternae, and swollen mitochondria in the electron-dense cytoplasm (Fig. 8b).

DISCUSSION

The finding of this study show that elevated IOP affects the sensitivity of both photoreceptors and RGCs, and that the invoked retinal damage progresses along two paths. Pressure-induced ischemic insult initiated from the outer retina propagates to the inner retina; and pressure-injured retrograde degeneration starting from the axon of RGCs in the optic-nerve head transfers to their soma in the inner retina. Interestingly, the two paths lead to apoptotic death of the photoreceptors and necrotic apoptosis of the RGCs.

In a full-field flash ERG, the a-wave reflects a massive response from the photoreceptors [11, 12, 17], whereas the b-wave, reflects the summed activity of ON-bipolar cells [18] with lateral input from horizontal cells [19], and an interaction of the ON-bipolar cells and the Müller cells [20]. Based on this in our study, a-wave amplitude changes that show significant reduction in scotopic and negligible reduction in photopic responses indicate that elevated IOP affects the rods and cones simultaneously. In the same manner, b-wave changes that show significant and less significant reduction in scotopic and in photopic responses, respectively, indicate that elevated pressure affects largely the rod function. In another rat glaucoma model, it has been reported that amplitude decreases were not significant prior to ~3 months of ocular hypertension [21]; and, in another model, a significant decrease in ERG amplitudes at 4 weeks was reported [22]. Together with the drastic reduction in 8-week glaucoma that we report here, all three reports show different critical time points probably due to differing modelling methods and evaluation criteria. Given our finding that apoptotic photoreceptors death with drastic a-wave amplitude reduction occurs in the last time point, it can be further deduced that sustained elevated pressure raises ischemic conditions, leading the sensitivity compromised photoreceptors to die via apoptosis. Evidences supporting this hypothesis have been sought in ischemic experiments [23-25]. Milder ischemia by permanent occlusion of the carotid arteries has been introduced to affect the outer retina more readily [23], whereas acute retinal ischemia by elevation of IOP to 120 mmHg led to marked reduction in a-wave amplitudes [24] and to apoptotic photoreceptor death [25]. Despite these results, the significant reduction in scotopic a-wave can be gener-

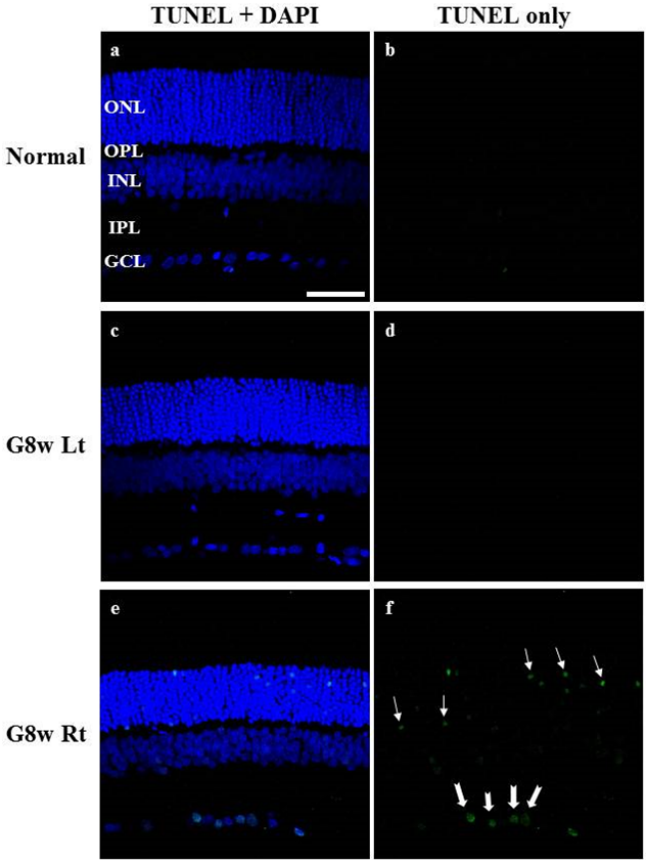

Fig. 7. Apoptotic cell death was evaluated via TUNEL. Left-side photographs (a, c, e), TUNEL+DAPI; right-side (b, d, f), TUNEL only. TUNEL-positive neurons appeared in the ganglion cell layer (GCL) (thick arrows) and in the outer nuclear layer (ONL) (thin arrows) in only 8-week glaucoma retina (G8w Rt: e, f). a & b, Normal; c & d, 8-week contralateral control retina (G8w Lt); INL, inner nuclear layer; IPL, inner plexiform layer; OPL, outer plexiform layer. Scale bar indicates 50 μm.

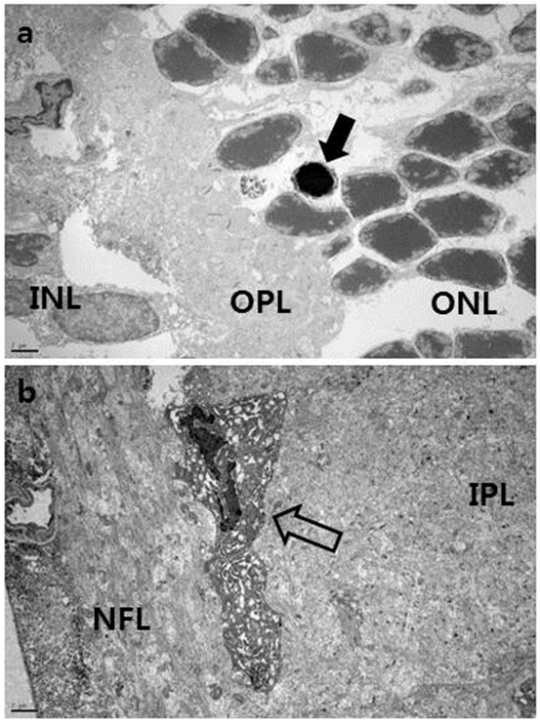

Fig. 8. Electron micrographs taken from 8-week glaucoma retina. In a, the apoptotic photoreceptor (closed arrow) appears in the outer nuclear layer (ONL). In b, the ganglion cell showing necrotic changes (opened arrow) is present. INL, inner nuclear layer; IPL, inner plexiform layer; NFL, nerve fibre layer; OPL, outer plexiform layer. Scale bars indicate 1 μm.

ally explained by the fact that rats have rod-dominant retinas, as documented by Osborne et al. [26]. There are, however, some clinical studies showing substantial glaucomatous damage to the outer retina. In flash ERGs of glaucoma patients, glaucomatous changes such as reductions and delays were larger and increased with disease severity [27], with a-wave amplitude significantly lowered [28]. With these results, the authors suggest that glaucomatous damage affects photoreceptors as well as RGCs due to both pressure stress and choroidal blood-flow insufficiency. Altogether, a-wave amplitude may be considered as a useful indicator for early detection of glaucoma degeneration.

PhNR in flash ERG has been previously suggested as an indicator in early diagnosis of glaucomatous optic neuropathy, wherein it was shown that PhNR drops even when visual sensitivity losses are mild in macaque glaucoma experiment [29]. Thereby, the authors concluded that PhNR arises from RGCs and their axons, but its delay could be mediated by glia. Another report describes significant decreases in PhNR amplitude with latency unaffected, occurring in early stages when IOP remarkably increased [11]. Largely in agreement with these results, our PhNR tracing showed significant reduction in the first week in only glaucoma and more remarkable reduction at 2 weeks in both retinas. It may therefore indicate that the earlier reduction means pressure-induced damage to the RGC sensitivity, and the later reduction in both retinas, additional damage to supportive glial structure in the optic-nerve head and its fast crossing-over to contralateral via electrical connection. The hypothesis of glial involvement was also consolidated by some morphological evidence from human glaucoma specimens and animal models. It has been found that elevation of IOP produces not only axonal changes, but also non-axonal pressure transducer, such as extracellular matrix and astrocytes, changes in the optic-nerve head [30]. On one hand, it was reported that astrocytes and Müller cells may be involved in the pathophysiology of RGC death or retinal repair in a rat model of acute ocular hypertension [31]. In addition, it has been more recently shown that astrocytes fortified by dense cytoskeletal filaments in the optic-nerve head are the target of raised IOP in rat glaucoma model [32]. Furthermore the

 https://doi.org/10.5607/en.2018.27.1.16

authors proposed that the damage in the axons is rather metabolic than mechanical, because of the localized loss of metabolic support for RGC axons from the astrocytes.

Because of the high energy requirement for crucial roles in photo-transduction, photoreceptors enrich numerous mitochondria in their inner segments, while RGCs do that in the global part of their axons [33]. Considering this, elevated-IOP-induced damage seems likely to affect both types of cell, causing mitochondrial dysfunction and invariably leading to apoptotic death. In accordance with this notion, we found that light-microscopically determined apoptosis occurred in photoreceptors, in addition to RGCs. However, apoptotic features of the two cell types were quite different in electron-microscopic observation, although direct matching with light microscopy is missing. Apoptotic features of photoreceptors were classical, whereas those of RGCs, nearly necrotic. Regarding the necrotic features of apoptotic RGCs, the death event of pressure-affected RGCs may be in agreement with the recently suggested theory of necrotic apoptosis or necroptosis [22, 34-36]. According to Degterev et al. [35], necroptosis occurs when death receptor-mediated extrinsic apoptosis pathway is triggered in the absence of intracellular apoptotic signaling, showing necrotic death morphology. On one hand, it has been suggested that necrosis might be regulated, showing the appearance of controlled apoptotic processes such as mitochondrial dysfunction, enhanced production of reactive oxygen species, and ATP depletion after damage-induced lesions [22, 36]. It was also shown that when essential apoptosis-regulating proteins are inhibited, the cell-death pathway could be shifted to necrosis, thereby demonstrating that different cell-death pathways cross-regulate each other [22]. In contrast, it was shown that the activation of death receptors leads to activated NF-κB to promote cell survival or to induce apoptosis and the third pathway, necroptosis [34]. The authors [34] also identified that a death-domain-containing kinase, receptor-interacting protein (RIP) 1 participates in all three cell-fate pathways. Based on these several lines of evidence [22, 34-36], we carefully suggest that RGC death affected by elevated IOP in rat might be caused by necrotic apoptosis as adjudged by necrotic morphology and DNA breakdown. This RGC death phenomenon might be caused by two routes: one is a direct effect of pressure on RGC axon in the retina, and the other is an indirect effect of pressure-injured astrocytes supporting RGC axons in the optic-nerve head.

Morphological evaluations of three kinds of calcium-binding proteins showed slightly different change patterns in both immunoreactivity and total protein amounts. Parvalbumin immunoreactivity in AII amacrine cells [37], showed more reduction in dendrites arborized near the GCL in 8-week glaucoma, without large change in protein levels. Considering the synaptic characteristics of AII amacrine cells [37], it may be indicated that the dendrites and ON cone bipolar cells are more susceptible than the lobular appendages and OFF cone bipolar cells, respectively, to pressure-induced damage. Calbindin and calretinin immunoreactivity in amacrine cells was clearly reduced during glaucoma, well in accordance with previously published results [38, 39]. Total protein levels of calbindin and calretinin in glaucomatous retinas, however, showed decrease and increase, respectively. In case of calbindin, the increase in protein levels in 8-week glaucoma may be due to upregulated expression not in horizontal cells but in the RGC axons. Published results that showed no change in the number of calbindin-immunoreactive horizontal cells in glaucoma [39] and in ischemic [40] retinas support this assumption. Similarly, the increase in calretinin protein levels may be caused by upregulated expression in RGC axons. Previously, it was reported that calbindin and calretinin may participate in delaying the onset of cell death [41], and have distinct function in localized calcium signaling in RGCs with clear compartmentalization, such as calretinin distribution close to the plasma membrane in the absence of calbindin [42]. Based on this, fast propagation of axonal damage to the control retina and calretinin overexpression in our study may suggest that axonal damage is worsened by neighboring cells, for example astrocytes.

The CaSR is synthesized and anchored in the rough ER, terminally glycosylated in the Golgi apparatus, and delivered to the plasma membrane to detect dynamic changes in extracellular calcium cationic concentration [43]. With regard to the CaSR's function, it is documented, on one hand, that an extracellular calcium signal produced in a neighboring cell by calcium cation mobilization could be detected in nearby cells expressing the CaSR [44], but on the contrary, that activated CaSR plays a role in the long-term control of apoptosis by protecting apoptotic cells [45]. Together, our results, showing reduction in CaSR immunoreactivity in glaucomatous RGCs soma despite increased protein levels, may indicate targeting of the protein from the rough ER to the plasma membrane to perform its roles in both intercellular communication and cell protection from apoptotic death in response to altered extracellular environment caused by glaucomatous stimuli.

ACKNOWLEDGEMENTS

We thank Drs. Sun-Sook Paik and Hong-Lim Kim for their excellent technical contributions. This study was supported by a grant from the Ministry of Knowledge Economy, Republic of Korea (10030022).

REFERENCES

1. Quigley HA (1996) Number of people with glaucoma worldwide. Br J Ophthalmol 80:389-393.
2. Gupta N, Weinreb RN (1997) New definitions of glaucoma. Curr Opin Ophthalmol 8:38-41.
3. Weinreb RN, Khaw PT (2004) Primary open-angle glaucoma. Lancet 363:1711-1720.
4. Quigley HA, Hohman RM (1983) Laser energy levels for trabecular meshwork damage in the primate eye. Invest Ophthalmol Vis Sci 24:1305-1307.
5. Yamamoto T, Kitazawa Y (1998) Vascular pathogenesis of normal-tension glaucoma: a possible pathogenetic factor, other than intraocular pressure, of glaucomatous optic neuropathy. Prog Retin Eye Res 17:127-143.
6. Quigley HA, Dunkelberger GR, Green WR (1989) Retinal ganglion cell atrophy correlated with automated perimetry in human eyes with glaucoma. Am J Ophthalmol 107:453-464.
7. Quigley HA, Broman AT (2006) The number of people with glaucoma worldwide in 2010 and 2020. Br J Ophthalmol 90:262-267.
8. Weymouth AE, Vingrys AJ (2008) Rodent electroretinography: methods for extraction and interpretation of rod and cone responses. Prog Retin Eye Res 27:1-44.
9. Nguyen CT, Vingrys AJ, Wong VH, Bui BV (2013) Identifying cell class specific losses from serially generated electroretinogram components. BioMed Res Int 2013:796362.
10. Bach M, Poloschek CM (2013) Electrophysiology and glaucoma: current status and future challenges. Cell Tissue Res 353:287-296.
11. ElGohary AA, Elshazly LH (2015) Photopic negative response in diagnosis of glaucoma: an experimental study in glaucomatous rabbit model. Int J Ophthalmol 8:459-464.
12. Kawamoto EM, Vivar C, Camandola S (2012) Physiology and pathology of calcium signaling in the brain. Front Pharmacol 3:61.
13. Hofer AM, Brown EM (2003) Extracellular calcium sensing and signalling. Nat Rev Mol Cell Biol 4:530-538.
14. Bandyopadhyay S, Tfelt-Hansen J, Chattopadhyay N (2010) Diverse roles of extracellular calcium-sensing receptor in the central nervous system. J Neurosci Res 88:2073-2082.
15. Yano S, Brown EM, Chattopadhyay N (2004) Calcium-sensing receptor in the brain. Cell Calcium 35:257-264.
16. Makous W (2004) Scotopic vision. In: The visual neurosciences (Chalupa LM, Werner JS, eds), pp 838-850. MIT Press, Cambridge, MA.
17. Jamison JA, Bush RA, Lei B, Sieving PA (2001) Characterization of the rod photoresponse isolated from the dark-adapted primate ERG. Vis Neurosci 18:445-455.
18. Stockton RA, Slaughter MM (1989) B-wave of the electroretinogram. A reflection of ON bipolar cell activity. J Gen Physiol 93:101-122.
19. Hanitzsch R, Küppers L, Flade A (2004) The effect of GABA and the GABA-uptake-blocker NO-711 on the b-wave of the ERG and the responses of horizontal cells to light. Graefes Arch Clin Exp Ophthalmol 242:784-791.
20. Dick E, Miller RF (1985) Extracellular K+ activity changes related to electroretinogram components. I. Amphibian (I-type) retinas. J Gen Physiol 85:885-909.
21. Mittag TW, Danias J, Pohorenec G, Yuan HM, Burakgazi E, Chalmers-Redman R, Podos SM, Tatton WG (2000) Retinal damage after 3 to 4 months of elevated intraocular pressure in a rat glaucoma model. Invest Ophthalmol Vis Sci 41:3451-3459.
22. Grozdanic SD, Betts DM, Sakaguchi DS, Kwon YH, Kardon RH, Sonea IM (2003) Temporary elevation of the intraocular pressure by cauterization of vortex and episcleral veins in rats causes functional deficits in the retina and optic nerve. Exp Eye Res 77:27-33.
23. Osborne NN, Safa R, Nash MS (1999) Photoreceptors are preferentially affected in the rat retina following permanent occlusion of the carotid arteries. Vision Res 39:3995-4002.
24. Chidlow G, Schmidt KG, Wood JP, Melena J, Osborne NN (2002) Alpha-lipoic acid protects the retina against ischemia-reperfusion. Neuropharmacology 43:1015-1025.
25. Singh M, Savitz SI, Hoque R, Gupta G, Roth S, Rosenbaum PS, Rosenbaum DM (2001) Cell-specific caspase expression by different neuronal phenotypes in transient retinal ischemia. J Neurochem 77:466-475.
26. Osborne NN, Casson RJ, Wood JP, Chidlow G, Graham M, Melena J (2004) Retinal ischemia: mechanisms of damage and potential therapeutic strategies. Prog Retin Eye Res 23:91-147.
27. Vaegan, Graham SL, Goldberg I, Buckland L, Hollows FC (1995) Flash and pattern electroretinogram changes with optic atrophy and glaucoma. Exp Eye Res 60:697-706.
28. Velten IM, Korth M, Horn FK (2001) The a-wave of the dark adapted electroretinogram in glaucomas: are photoreceptors affected? Br J Ophthalmol 85:397-402.
29. Viswanathan S, Frishman LJ, Robson JG, Harwerth RS, Smith EL 3rd (1999) The photopic negative response of the macaque electroretinogram: reduction by experimental glaucoma. Invest Ophthalmol Vis Sci 40:1124-1136.
30. Morrison JC, Johnson EC, Cepurna W, Jia L (2005) Under-

https://doi.org/10.5607/en.2018.27.1.16

standing mechanisms of pressure-induced optic nerve damage. Prog Retin Eye Res 24:217-240.
31. Lam TT, Kwong JM, Tso MO (2003) Early glial responses after acute elevated intraocular pressure in rats. Invest Ophthalmol Vis Sci 44:638-645.
32. Dai C, Khaw PT, Yin ZQ, Li D, Raisman G, Li Y (2012) Structural basis of glaucoma: the fortified astrocytes of the optic nerve head are the target of raised intraocular pressure. Glia 60:13-28.
33. Osborne NN (2010) Mitochondria: their role in ganglion cell death and survival in primary open angle glaucoma. Exp Eye Res 90:750-757.
34. Christofferson DE, Yuan J (2010) Necroptosis as an alternative form of programmed cell death. Curr Opin Cell Biol 22:263-268.
35. Degterev A, Huang Z, Boyce M, Li Y, Jagtap P, Mizushima N, Cuny GD, Mitchison TJ, Moskowitz MA, Yuan J (2005) Chemical inhibitor of nonapoptotic cell death with therapeutic potential for ischemic brain injury. Nat Chem Biol 1:112-119.
36. Hitomi J, Christofferson DE, Ng A, Yao J, Degterev A, Xavier RJ, Yuan J (2008) Identification of a molecular signaling network that regulates a cellular necrotic cell death pathway. Cell 135:1311-1323.
37. Rodieck RW (1998) The first steps in seeing. Sinauer Associates, Sunderland, MA.
38. Hernandez MR (2000) The optic nerve head in glaucoma: role of astrocytes in tissue remodeling. Prog Retin Eye Res 19:297-321.
39. Gunn DJ, Gole GA, Barnett NL (2011) Specific amacrine cell changes in an induced mouse model of glaucoma. Clin Exp Ophthalmol 39:555-563.
40. Chun MH, Kim IB, Ju WK, Kim KY, Lee MY, Joo CK, Chung JW (1999) Horizontal cells of the rat retina are resistant to degenerative processes induced by ischemia-reperfusion. Neurosci Lett 260:125-128.
41. D'Orlando C, Fellay B, Schwaller B, Salicio V, Bloc A, Gotzos V, Celio MR (2001) Calretinin and calbindin D-28k delay the onset of cell death after excitotoxic stimulation in transfected P19 cells. Brain Res 909:145-158.
42. Mojumder DK, Wensel TG, Frishman LJ (2008) Subcellular compartmentalization of two calcium binding proteins, calretinin and calbindin-28 kDa, in ganglion and amacrine cells of the rat retina. Mol Vis 14:1600-1613.
43. Bouschet T, Martin S, Henley JM (2008) Regulation of calcium-sensing-receptor trafficking and cell-surface expression by GPCRs and RAMPs. Trends Pharmacol Sci 29:633-639.
44. Hofer AM, Curci S, Doble MA, Brown EM, Soybel DI (2000) Intercellular communication mediated by the extracellular calcium-sensing receptor. Nat Cell Biol 2:392-398.
45. Brown EM, MacLeod RJ (2001) Extracellular calcium sensing and extracellular calcium signaling. Physiol Rev 81:239-297.